

Structure and Dynamics of a Trinuclear Gadolinium(III) Complex: The Effect of Intramolecular Electron Spin Relaxation on Its Proton Relaxivity¹

Éva Tóth,[†] Lothar Helm,[†] André E. Merbach,^{*,‡} Roman Hedinger,[‡]
Kaspar Hegetschweiler,^{*,§} and András Jánosy^{*,||}

Institute of Inorganic and Analytical Chemistry, University of Lausanne, Switzerland, Laboratorium für Anorganische Chemie, ETH-Zentrum, Zürich, Switzerland, Universität des Saarlandes, Fachrichtung Anorganische Chemie, Saarbrücken, Germany, and Department of Experimental Physics, Technical University of Budapest, Hungary

Received February 6, 1998

The trinuclear $[\text{Gd}_3(\text{H}_3\text{taci})_2(\text{H}_2\text{O})_6]^{3+}$ complex has been characterized in aqueous solution as a model compound from the point of view of MRI: the parameters that affect proton relaxivity have been determined in a combined variable temperature, pressure, and multiple-field ¹⁷O NMR, EPR, and NMRD study. The solution structure of the complex was found to be the same as in solid state: the total coordination number of the lanthanide(III) ion is 8 with two inner-sphere water molecules. EPR measurements proved a strong intramolecular dipole–dipole interaction between Gd(III) electron spins. This mechanism dominates electron spin relaxation at high magnetic fields ($B > 5$ T). Its proportion to the overall relaxation decreases with decreasing magnetic field and becomes a minor term at fields used in MRI. Consequently, it cannot increase the electronic relaxation rates to such an extent that they limit proton relaxivity. $[\text{Gd}_3(\text{H}_3\text{taci})_2(\text{H}_2\text{O})_6]^{3+}$ undergoes a relatively slow water exchange ($k_{\text{ex}}^{298} = (1.1 \pm 0.2) \times 10^7 \text{ s}^{-1}$) compared to the Gd(III) aqua ion, while the mechanism is much more associatively activated as shown by the activation volume ($\Delta V^\ddagger = (-12.7 \pm 1.5) \text{ cm}^3 \text{ mol}^{-1}$). The lower exchange rate, as compared to $[\text{Gd}(\text{H}_2\text{O})_8]^{3+}$ and $[\text{Gd}(\text{PDTA})(\text{H}_2\text{O})_2]^-$, can be explained with the higher rigidity of the $[\text{Gd}_3(\text{H}_3\text{taci})_2(\text{H}_2\text{O})_6]^{3+}$ which considerably slows down the transition from the eight-coordinate reactant to the nine-coordinate transition state. The unexpectedly low rotational correlation time of the complex is interpreted in terms of a spherical structure with a large hydrophobic surface avoiding the formation of a substantial hydration sphere around $[\text{Gd}_3(\text{H}_3\text{taci})_2(\text{H}_2\text{O})_6]^{3+}$.

Introduction

The ligand 1,3,5-triamino-1,3,5-trideoxy-*cis*-inositol (taci; Scheme 1) is able to form complexes with practically all metal ions, as demonstrated in a series of recent publications.^{2–7} This versatility is due to the four different binding sites which allow the coordination of a metal ion to three nitrogen atoms (coordination mode 1 in Scheme 1), one oxygen and two nitrogen atoms (coordination mode 2), one nitrogen and two oxygen atoms (coordination mode 3), or three oxygen atoms (coordination mode 4), depending on the softness and size of the metal. Furthermore, the ligand is able to coordinate in

different tautomeric forms providing either alkoxo or hydroxyl groups for metal binding.

With lanthanide(III) ions trinuclear $[\text{Gd}_3(\text{H}_3\text{taci})_2(\text{H}_2\text{O})_6]\text{Cl}_3 \cdot 3.5\text{H}_2\text{O}$, $[\text{Eu}_3(\text{H}_3\text{taci})_2(\text{H}_2\text{O})_6](\text{NO}_3)_3 \cdot 3\text{H}_2\text{O}$, and $[\text{La}_3(\text{H}_3\text{taci})_2(\text{H}_2\text{O})_4\text{Cl}]\text{Cl}_2 \cdot 3\text{H}_2\text{O}$ complexes have been obtained as solids.^{8–10} The X-ray crystallographic analysis revealed a very compact structure and extremely short metal–metal distances (Gd–Gd, 3.7 Å; Eu–Eu, 3.8 Å; La–La, 3.9 Å). A representation of the Gd complex can be seen in Chart 1. Magnetic susceptibility measurements on this complex showed antiferromagnetic behavior in the temperature range 2.3–60 K, with a weak coupling constant of $J = -0.092 \text{ cm}^{-1}$.^{9,10} pH potentiometry has been used to investigate the stability of several lanthanide^{III}–taci complexes in aqueous solution.^{9,10} Potentiometric measurements suggested the presence of trinuclear complexes having the same composition in solution as in the solid state at pH > 6.5. The solution structure was confirmed by a ¹H NMR study on the Eu complex.^{9,10}

* To whom correspondence should be addressed.

[†] University of Lausanne.

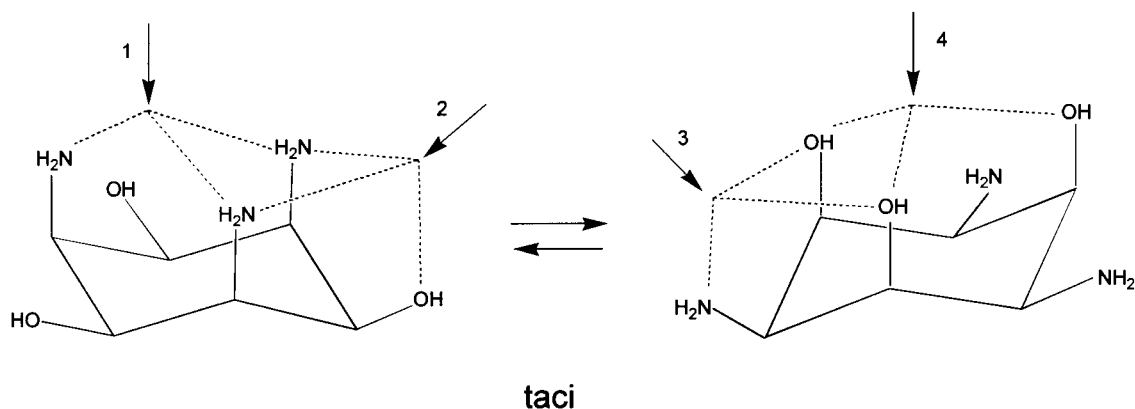
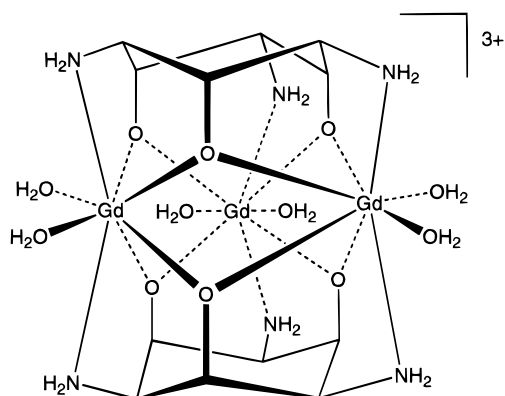
[‡] ETH.

[§] Universität des Saarlandes.

^{||} Technical University of Budapest.

- (1) Part 86 of the series High Pressure NMR Kinetics. Part 85: Tóth, É.; van Uffelen, I.; Helm, L.; Merbach, A. E.; Ladd, D.; Briley-Sæbø K.; Kellar, K. E. *Magn. Reson. Chem.* **1998**, *36*, 5125.
- (2) Schmalte, H. W.; Hegetschweiler, K.; Ghisletta, M. *Acta Crystallogr.* **1991**, *C47*, 2047.
- (3) Hegetschweiler, K.; Gramlich, V.; Ghisletta, M.; Samaras, H. *Inorg. Chem.* **1992**, *31*, 2341.
- (4) Ghisletta, M.; Jalett, H.-P.; Gerfin, T.; Gramlich, V.; Hegetschweiler, K. *Helv. Chim. Acta* **1992**, *75*, 2233.
- (5) Hegetschweiler, K.; Ghisletta, M.; Fässler, T. F.; Nesper, R.; Schmalte, H. W.; Rihs, G. *Inorg. Chem.* **1993**, *32*, 2032.
- (6) Hegetschweiler, K.; Hancock, R. D.; Ghisletta, M.; Kradolfer, T.; Gramlich, V.; Schmalte, H. W. *Inorg. Chem.* **1993**, *32*, 5273.
- (7) Hegetschweiler, K.; Ghisletta, M.; Gramlich, V. *Inorg. Chem.* **1993**, *32*, 2699.

- (8) Ghisletta, M. 1,3,5-Triamino-1,3,5-trideoxy-*cis*-inositol—Synthese des Liganden und Bildung von Komplexen mit verschiedenen Metallen. Doctoral Thesis, No. 10891, ETH, Zurich, 1994.
- (9) Hedinger, R. Die *N,N,O*-Bindungsstelle von 1,3,5-Triamino-1,3,5-trideoxy-*cis*-inositol und 1,3,5-Trisdesoxy-1,3,5-tris(dimethylamino)-*cis*-inositol. Koordinationschemische Studien an Ln(III)-, Pb(II)-, und Re(I)-Komplexen. Doctoral Thesis, No. 12611, ETH, Zurich, 1998.
- (10) Hedinger, R.; Ghisletta, M.; Hegetschweiler, K.; Tóth, É.; Merbach, A. E.; Sessoli, R.; Gatteschi, D.; Gramlich, V. Submitted for publication.
- (11) Lauffer, R. B. *Chem. Rev.* **1987**, *87*, 901.

Scheme 1. Coordination Modes of Taci**Chart 1.** Representation of $[\text{Gd}_3(\text{H}_3\text{-taci})_2(\text{H}_2\text{O})_6]^{3+}$, Drawn after the Solid State Structure

Gd^{III} -poly(aminocarboxylate) complexes are widely utilized as contrast enhancing agents in magnetic resonance imaging.^{11,12} Their efficacy, quantified as proton relaxivity, is given by their ability to decrease the relaxation time of the surrounding water protons. Proton relaxivity is determined by several factors, including the longitudinal and transverse relaxation rates of the Gd electron spin. In the case of Gd(III), electron spin relaxation in solution is mainly governed by a transient zero-field splitting mechanism.¹³ When two or more Gd(III) ions are in close proximity, an additional relaxation mechanism arises from intramolecular dipole-dipole interactions between the Gd(III) electron spins and results in increased relaxation rates compared to a corresponding monomeric complex. This phenomenon has been recently observed at high magnetic fields for dimeric Gd(III) poly(aminocarboxylates).¹⁴ Since slow rotation of the contrast agent is favorable for proton relaxivity, one important approach in contrast agent development has been in increasing the size of the molecule by synthesizing dimeric or polymeric complexes. In these complexes, the Gd(III) ions may be situated relatively close to each other which should result in increased electron spin relaxation through intramolecular dipole-dipole interactions.

For currently used Gd-based contrast agents, proton relaxivity is not limited by electronic relaxation. In this study our objective was to investigate if electronic relaxation can be accelerated to such an extent by the intramolecular dipole-dipole coupling that it starts to limit proton relaxivity. Experi-

mental data on this subject are not available. The trinuclear Gd(III) complex of taci is a good model since the three metal ions are very close to each other, thus a strong interaction can be expected between them. These interactions become proportionally more significant at high magnetic fields, necessitating a high field EPR study.

In this paper we report the characterization of $[\text{Gd}_3(\text{H}_3\text{-taci})_2(\text{H}_2\text{O})_6]^{3+}$, as a model compound, in aqueous solution from the point of view of MRI, even if its stability does not allow to envisage its use for this purpose. A variable temperature, pressure, multiple field ^{17}O NMR and EPR and a variable temperature NMRD study have been performed and the data were analyzed in terms of water exchange dynamics and rotation (NMRD = nuclear magnetic relaxation dispersion, which measures proton relaxivity as a function of the magnetic field).

Experimental Section

Preparation of the Complexes. The ligand taci and the Ln(III) complexes were prepared according to refs 4 and 9, respectively. The complexes were dissolved in double distilled water, and the pH, measured with a combined glass electrode, was adjusted by adding weighed amounts of aqueous solutions of perchloric acid or sodium hydroxide of known concentration. The pH of the solutions was always chosen on the basis of the stability constants so that the only species present is the $[\text{Ln}_3(\text{H}_3\text{-taci})_2(\text{H}_2\text{O})_6]^{3+}$ complex.^{9,10} ^{17}O -enriched water (Yeda R&D Co., Rehovot, Israel) was added to the solutions for ^{17}O NMR measurements to improve sensitivity (final enrichment ca. 2%).

UV-Visible Spectrophotometry. UV-visible spectra were recorded for a $[\text{Eu}_3(\text{H}_3\text{-taci})_2(\text{H}_2\text{O})_6]^{3+}$ solution ($c_{\text{Eu}} = 0.017 \text{ M}$; pH = 7.4) in the temperature range 10–75 °C on a Perkin-Elmer Lambda 19 spectrometer, in thermostatable cells with a 10 cm optical length ($\lambda = 578\text{--}582 \text{ nm}$).

^{17}O NMR Measurements. A variable-temperature ^{17}O NMR study on $[\text{Gd}_3(\text{H}_3\text{-taci})_2(\text{H}_2\text{O})_6]^{3+}$ was performed at four different magnetic fields using Bruker spectrometers: AMX2-600, 14.1 T, 81.4 MHz; AM-400, 9.4 T; 54.2 MHz; 1.41 T, 8.14 MHz; and 0.572 T, 3.3 MHz electromagnets connected to a AC-200 console. Bruker VT-1000 temperature control units were used to stabilize the temperature, which was measured by a substitution technique.¹⁵ The samples were sealed in glass spheres and placed in 10 mm NMR tubes to eliminate susceptibility effects. Bulk water longitudinal relaxation rates, $1/T_1$, were obtained by the inversion recovery method,¹⁶ and transverse relaxation rates, $1/T_2$, by the Carr-Purcell-Meiboom-Gill spin-echo technique,¹⁷ or, for line widths greater than 500 Hz, directly from the line widths. The measurements were performed at different concentrations ($c_{\text{Gd}} = 0.04\text{--}0.1 \text{ M}$; pH = 7.4) in order to exclude possible

(12) Peters, J. A.; Huskens, J.; Raber, D. J. *Prog. Nucl. Magn. Reson. Spectrosc.* **1996**, *28*, 283.

(13) McLachlan, A. D. *Proc. R. Soc. London* **1964**, *A280*, 271.

(14) Powell, H. D.; Ni Dhubghaill, O. M.; Pubanz, D.; Lebedev, Y.; Schlaepfer, W.; Merbach, A. E. *J. Am. Chem. Soc.* **1996**, *118*, 9333.

(15) Amman, C.; Meier, P.; Merbach, A. E. *J. Magn. Res.* **1982**, *46*, 319.

(16) Vold, R. V.; Waugh, J. S.; Klein, M. P.; Phelps, D. E. *J. Chem. Phys.* **1968**, *48*, 3831.

(17) Meiboom, S.; Gill, D. *Rev. Sci. Instrum.* **1958**, *29*, 688.

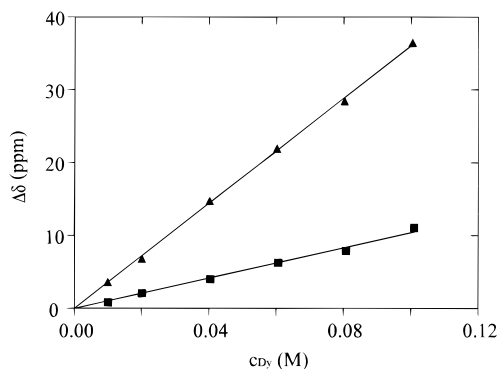


Figure 1. Plots of the Dy(III)-induced water ^{17}O shifts versus the Dy(III) concentration for solutions of $[\text{Dy}(\text{H}_2\text{O})_8]^{3+}$ (▲) and $[\text{Dy}_3(\text{H}-_3\text{taci})_2(\text{H}_2\text{O})_6]^{3+}$ (■). $T = 35\text{ }^\circ\text{C}$; $\text{pH} = 7.4$.

artifacts due to concentration effects. Under these conditions all Gd(III) (>99.5%) is in the form of the complex. A solution of $[\text{Y}_3(\text{H}-_3\text{taci})_2(\text{H}_2\text{O})_6]^{3+}$ of the same concentration and pH was used as reference.

Variable-pressure NMR spectra were recorded up to a pressure of 200 MPa on a Bruker AM-400 spectrometer equipped with a home-built high-pressure probe.¹⁸ The temperature was controlled by a circulating fluid from an external temperature bath and measured with a built-in Pt resistor.

The dysprosium induced shift measurements were performed on a Bruker AM-400 spectrometer at 35 $^\circ\text{C}$. ^{17}O -enriched nitromethane was used as an internal chemical shift reference.¹⁹

EPR Measurements. The X-band (0.34 T) EPR spectra were recorded on a Bruker ESP 300E spectrometer, operating in continuous wave mode. The samples were placed in 1 mm quartz tubes. The cavity temperature was stabilized using electronic temperature control of gas flowing through the cavity and measured by substituting a thermometer for the sample tube.

The EPR spectra at $B = 2.7\text{ T}$ (resonance frequency 75 GHz) and 8.09 T (225 GHz) were measured on a home-built spectrometer.²⁰ The microwave source is a quartz-stabilized Gunn diode oscillator (Radiometer Physics) operating at 75 GHz, followed by a frequency tripler for the 225 GHz measurements. The temperature was stabilized with an Oxford Instruments ITC 502 control unit ($\pm 0.1\text{ K}$) and measured with a Pt resistor built into the probehead.

NMRD. The $1/T_1$ nuclear magnetic relaxation dispersion (NMRD) profiles of the solvent protons at 25 and 50 $^\circ\text{C}$ were obtained on a Spinmaster FFC fast field cycling NMR relaxometer (Stellar), covering a continuum of magnetic fields from 7×10^{-4} to 0.47 T (corresponding to a proton Larmor frequency range 0.03–20 MHz). The temperature was stabilized with a Stellar VTC90 control unit and measured by a substitution technique.¹⁵

Data Analysis. All the data (including the simultaneous least-squares fit of EPR, ^{17}O NMR, and NMRD data) were fitted by the program Scientist for Windows by Micromath, version 2.0. The reported errors correspond to one standard deviation obtained by statistical analysis.

Results

Dy(III)-Induced Water ^{17}O Shifts. Addition of the $[\text{Dy}_3(\text{H}-_3\text{taci})_2]^{3+}$ complex to water results in a shift of the water ^{17}O NMR signal to lower frequencies (Figure 1). The exchange of water between the Dy(III) complex and the bulk is fast on the ^{17}O NMR time scale under the conditions applied. Previously, the Dy(III)-induced oxygen shifts were shown to be independent of the other ligands chelated to the Dy(III) ion and

to be predominantly contact in origin.²¹ Consequently, the slope of a plot of the Dy(III)-induced shift versus the Dy(III) concentration is proportional to the hydration number of the Dy(III) complex. A comparison of the slopes of the plots obtained for the eight-coordinate^{22,23} $[\text{Dy}(\text{H}_2\text{O})_8]^{3+}$ and $[\text{Dy}_3(\text{H}-_3\text{taci})_2]^{3+}$ yields a value of 2.3 ± 0.1 for the number of coordinated water molecules per Dy in the taci complex.

UV–Vis Measurements. The $^7\text{F}_0 \rightarrow ^5\text{D}_0$ transition band of the Eu^{3+} ion is very sensitive to changes in the coordination environment. It is a useful probe to check the presence of differently solvated complexes in solution, as was shown for several poly(aminocarboxylate) complexes.^{24,25} A single absorption band was observed for the $[\text{Eu}_3(\text{H}-_3\text{taci})_2(\text{H}_2\text{O})_6]^{3+}$ aqueous solution in the temperature range studied, thus excluding the presence of any hydration equilibria.

EPR, ^{17}O NMR, and NMRD Measurements on $[\text{Gd}_3(\text{H}-_3\text{taci})_2(\text{H}_2\text{O})_6]^{3+}$. **Variable Temperature, Multiple-Field EPR Measurements.** The line shapes at all fields were approximately Lorentzian. The overall transverse electronic relaxation rates, $1/T_{2e}$, were obtained from the peak-to-peak EPR line widths of the derivative spectrum.²⁶

The electron spin relaxation rates for Gd(III) complexes are usually interpreted in terms of a transient zero-field splitting mechanism (ZFS), induced by distortions of the complex. The ZFS terms can be expressed by eqs 1 and 2,^{13,27} where Δ^2 is the trace of the square of the zero-field splitting tensor, τ_v is the correlation time for the modulation of the ZFS with the activation energy E_v and ω_s is the Larmor frequency of the Gd^{3+} electron spin:

$$\left(\frac{1}{T_{1e}}\right)^{\text{ZFS}} = \frac{1}{25} \Delta^2 \tau_v \{4S(S+1) - 3\} \left\{ \frac{1}{1 + \omega_s^2 \tau_v^2} + \frac{4}{1 + 4\omega_s^2 \tau_v^2} \right\} \quad (1)$$

$$\left(\frac{1}{T_{2e}}\right)^{\text{ZFS}} = \Delta^2 \tau_v \left[\frac{5.26}{1 + 0.372\omega_s^2 \tau_v^2} + \frac{7.18}{1 + 1.24\omega_s^2 \tau_v^2} \right] \quad (2)$$

$$\tau_v = \tau_v^{298} \exp\left\{ \frac{E_v}{R} \left(\frac{1}{T} - \frac{1}{298.15} \right) \right\} \quad (3)$$

In previous studies on Gd(III) complexes a magnetic field independent spin rotation (SR) relaxation mechanism was also included (eq 4), though it represents only a very small contribution to the total relaxation.²⁸ It is quantified by the deviations from the free electron g_L value (δg_L^2).

$$\left(\frac{1}{T_{1e}}\right)^{\text{SR}} = \frac{\delta g_L^2}{9\tau_R} \quad (4)$$

(18) Frey, U.; Helm, L.; Merbach, A. E. *High Press. Res.* **1990**, *2*, 237.

(19) Sandler, S. R.; Karo, W. *Organic Functional Group Preparations*; Academic Press: New York, 1968; Vol. 1, p 425.

(20) Fehér, T. MS Diploma Work, Department of Experimental Physics, Technical University of Budapest, 1997.

(21) Alpoim, M. C.; Urbano, A. M.; Gerales, C. F. C. G.; Peters, J. A. J. *Chem. Soc., Dalton Trans.* **1992**, 463 and references therein.

(22) Cossy, C.; Barnes, A. C.; Enderby, J. E.; Merbach, A. E. *J. Chem. Phys.* **1988**, *90*, 3254.

(23) Kowall, Th.; Foglia, F.; Helm, L.; Merbach, A. E. *J. Am. Chem. Soc.* **1995**, *117*, 3790.

(24) Geier, G.; Jorgensen, C. K. *Chem. Phys. Lett.* **1971**, 263.

(25) Graeppl, N.; Powell, D. H.; Laurenczy, G.; Zékány, L.; Merbach, A. E. *Inorg. Chim. Acta*, **1994**, *235*, 311.

(26) Reuben, J. J. *J. Phys. Chem.* **1971**, *75*, 3164.

(27) Powell, D. H.; Merbach, A. E.; González, G.; Brücher, E.; Micskei, K.; Ottaviani, M. F.; Köhler, K.; von Zelewsky, A.; Grinberg, O. Y.; Lebedev, Y. S. *Helv. Chim. Acta* **1993**, *76*, 2129.

(28) Gonzalez, G.; Powell, D. H.; Tissières, V.; Merbach, A. E. *J. Phys. Chem.* **1994**, *98*, 53.

Besides the zero-field splitting and spin rotation mechanisms, for the trinuclear $[\text{Gd}_3(\text{H}_3\text{taci})_2(\text{H}_2\text{O})_6]^{3+}$, the relaxation caused by the mutual dipolar coupling of three identical spins placed at the corners of an equilateral triangle will be considered as a crude approximation.²⁹ This approximation can be justified by the relative strength of the ZFS energy, which is in the order of $0.2\text{--}0.4\text{ cm}^{-1}$ for Gd(III) complexes,¹⁴ compared to the dipolar coupling of $J_{\text{dip}} = g^2\mu^2r^{-3} = 0.033\text{ cm}^{-1}$ ($r = 3.734\text{ \AA}$).¹⁰ Intramolecular dipole–dipole interaction between the three $7/2$ spins is approximated by Abragam's equations for like spin pairs.³⁰ These equations are strictly valid only for $I = 1/2$ spins but can be used as approximation for $I > 1/2$ provided $\hbar\omega_0 \ll kT$.³¹ Strictly speaking, these equations are only valid provided the motion of the spins is not correlated. In eqs 5 and 6 J_n^{intra} is the spectral density function, defined by eq 7, and r_{GdGd} is the intramolecular Gd–Gd distance.

$$\left(\frac{1}{T_{1e}}\right)^{\text{intra}} = \frac{2}{5} \left(\frac{\mu_0}{4\pi}\right)^2 \frac{\hbar^2 \gamma_S^4 S(S+1)}{r_{\text{GdGd}}^6} (2J_1^{\text{intra}} + 8J_2^{\text{intra}}) \quad (5)$$

$$\left(\frac{1}{T_{2e}}\right)^{\text{intra}} = \frac{2}{5} \left(\frac{\mu_0}{4\pi}\right)^2 \frac{\hbar^2 \gamma_S^4 S(S+1)}{r_{\text{GdGd}}^6} (3J_0^{\text{intra}} + 5J_1^{\text{intra}} + 2J_2^{\text{intra}}) \quad (6)$$

$$J_n^{\text{intra}} = \frac{\tau_{\text{Re}}}{1 + n^2 \omega_S^2 \tau_{\text{Re}}^2} \quad (7)$$

The correlation time, τ_{Re} , is assumed to have a simple exponential temperature dependence (eq 8) with value τ_{Re}^{298} at 298.15 K and E_{Re} as activation energy.

$$\tau_{\text{Re}} = \tau_{\text{Re}}^{298} \exp\left\{\frac{E_{\text{Re}}}{R}\left(\frac{1}{T} - \frac{1}{298.15}\right)\right\} \quad (8)$$

The proportion of the intramolecular dipole–dipole relaxation mechanism compared to the two other contributions (zero-field splitting and spin rotation) is larger at high magnetic fields. Therefore, the most reliable information on this mechanism can best be obtained at the highest field. The transverse electronic relaxation rates measured in aqueous solutions of $[\text{Gd}_3(\text{H}_3\text{taci})_2(\text{H}_2\text{O})_6]^{3+}$ of four different Gd concentrations at 8.09 T are presented in Figure 2. As a comparison, the transverse relaxation rates obtained at 8.09 T for a typical monomer Gd(III) complex, $[\text{Gd}(\text{DTPA-BMA})]$, are also shown (DTPA-BMA = 1,7-bis(*N*-methylcarbamoyl)methyl)-1,4,7-tris(carboxymethyl)-1,4,7-triazaheptane). As expected, the electronic relaxation is much faster in the case of the trinuclear $[\text{Gd}_3(\text{H}_3\text{taci})_2(\text{H}_2\text{O})_6]^{3+}$. Certainly, for a correct comparison one would need a monomer complex of a similar symmetry. However, since the monomer Gd(III) complexes studied so far do not differ so much in terms of electronic relaxation,¹⁴ this comparison can illustrate well the difference between monomers in general and the trimer

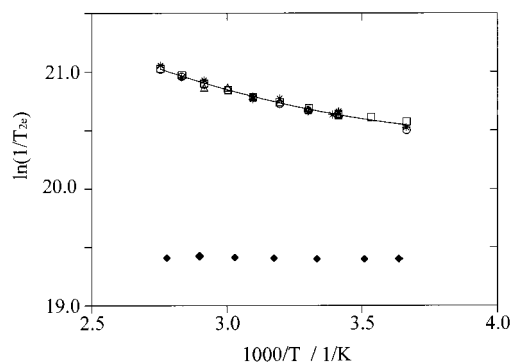


Figure 2. Temperature dependence of the transverse electronic relaxation rates at 8.09 T in $[\text{Gd}_3(\text{H}_3\text{taci})_2(\text{H}_2\text{O})_6]^{3+}$ solutions ($c_{\text{Gd}} = 0.06$ (□); 0.04 (○); 0.02 (△), 0.009 M (*)) and in a Gd(DTPA-BMA) solution ($c_{\text{Gd}} = 0.08$ M (◆)). The curve corresponds to the fit of the data as described in the text.

Table 1. Parameters Obtained from the Analysis of the Variable-Temperature, High-Field EPR Data

	$\tau_{\text{Re}}^{298}/\text{ps}$	$E_{\text{Re}}/\text{kJ mol}^{-1}$	$r_{\text{GdGd}}/\text{\AA}$
$[\text{Gd}_3(\text{H}_3\text{taci})_2(\text{H}_2\text{O})_6]^{3+}$	0.3 ± 0.05	1.0^c	3.7
$[\text{pip}\{\text{Gd}(\text{DO3A})(\text{H}_2\text{O})_2\}_2]^a$	185 ± 30	8.2 ± 5	8.7
$[\text{bisoxa}\{\text{Gd}(\text{DO3A})(\text{H}_2\text{O})_2\}_2]^b$	163 ± 40	5 ± 7	9.3

^a $\text{pip}(\text{DO3A})_2 = \text{bis}(1,4\text{-}(1\text{-}(\text{carboxymethyl})\text{-}1,4,7,10\text{-tetraaza-}4,7,10\text{-tris}(\text{carboxymethyl})\text{-}1\text{-cyclododecyl})\text{-}1,4\text{-diazacyclohexane}$. ^b $\text{Bisoxa}(\text{DO3A})_2 = \text{bis}(1,4\text{-}(1\text{-}(\text{carboxymethyl})\text{-}1,4,7,10\text{-tetraaza-}4,7,10\text{-tris}(\text{carboxymethyl})\text{-}1\text{-cyclododecyl})\text{-}1,10\text{-diazacyclohexane}$. ^c The activation energy was fixed in the fitting procedure.

$[\text{Gd}_3(\text{H}_3\text{taci})_2(\text{H}_2\text{O})_6]^{3+}$. Previous studies on Gd(III) complexes showed an important concentration dependence of the transverse electronic relaxation rates at high magnetic field (5 T).^{14,27} The linear increase of the relaxation rates with the Gd(III) concentration was explained in terms of an intermolecular dipole–dipole relaxation mechanism. For $[\text{Gd}_3(\text{H}_3\text{taci})_2(\text{H}_2\text{O})_6]^{3+}$ no concentration dependence was found which indicates that intermolecular effects are negligible compared to intramolecular interactions.

In the fits, the relaxation rate due to the zero-field splitting and spin rotation mechanisms—both representing only a minor contribution at high field—were described in one term, $(1/T_{2e})^0$. Thus we have fitted the 8.09 T EPR data by assuming that the total relaxation rate is the sum of $(1/T_{2e})^0$ and $(1/T_{2e})^{\text{intra}}$, and that $(1/T_{2e})^0$ has an exponential temperature dependence with value $(1/T_{2e})^{0,298}$ at 298.15 K and E_0 as activation energy (eq 9). Since no concentration dependence was found, the relaxation

$$\left(\frac{1}{T_{2e}}\right)^0 = \left(\frac{1}{T_{2e}}\right)^{0,298} \exp\left\{\frac{E_0}{R}\left(\frac{1}{298.15} - \frac{1}{T}\right)\right\} \quad (9)$$

rates measured at different Gd(III) concentrations were fitted together. The Gd–Gd distance was estimated from the X-ray structure of the complex. The line in Figure 2 represents the fitted function and the correlation time obtained is shown and compared to those for Gd-dimers in Table 1. The value of the activation energy was fixed to 1 kJ mol^{-1} , otherwise, when fitted, the fit resulted in a small negative value.

Variable-Temperature ¹⁷O NMR. The reduced relaxation rates, $1/T_{1r}$, $1/T_{2r}$, and chemical shift, $\Delta\omega_r$, were calculated from the measured ¹⁷O NMR relaxation rates and chemical shifts of the paramagnetic solutions and of the reference (relevant equations are given in Appendix). Outer-sphere contributions to the ¹⁷O-reduced relaxation rates are negligible. The longitudinal relaxation rates in Gd^{3+} solutions are dominated by

(29) This analysis can be justified by the small value of the coupling constant determined by magnetic susceptibility measurements ($J = -0.092\text{ cm}^{-1}$). The analysis within this approximation is internally consistent but not unique. Other approaches could be used to address some aspects of the evaluation of the experimental data, such as the problem of rotational correlation, electron relaxation when the electron spins are correlated, etc. Such analysis, which raises difficult physical problems that may not be solved by simple approaches, is reserved for the future with complementary experimental data.

(30) Abragam, A. *The Principles of Nuclear Magnetism*; Oxford University Press: London, 1961.

(31) McConnell, J. *Nuclear Magnetic Relaxation in Liquids*; Cambridge University Press: Cambridge, 1987; pp 56–59.

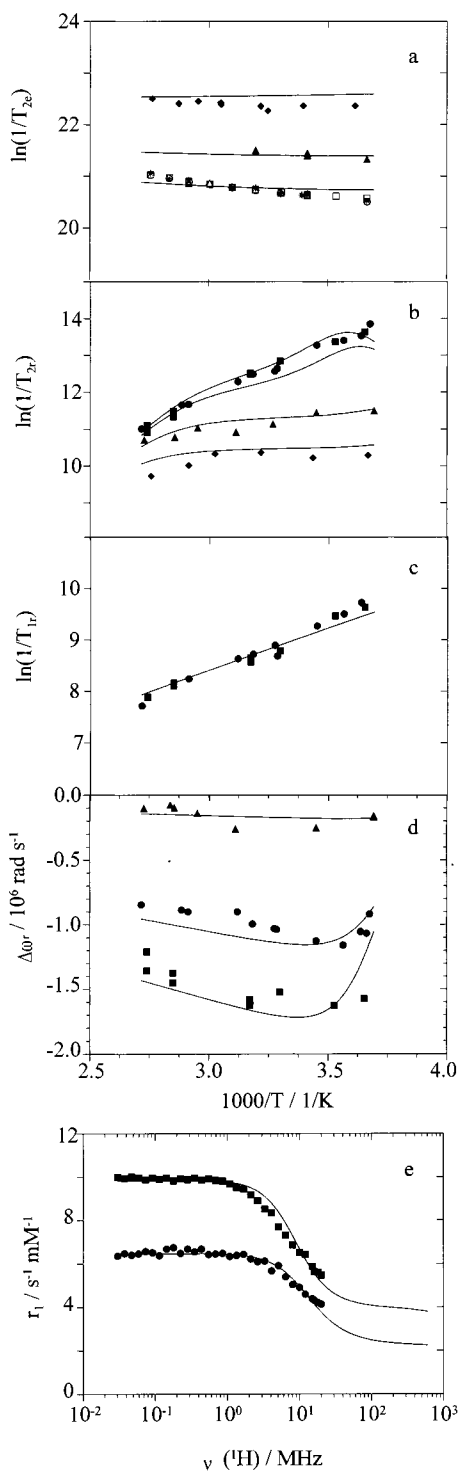


Figure 3. Temperature dependence of (a) transverse electronic relaxation rates at 0.34 (\diamond), 2.69 (+), and 8.09 T, $c_{\text{Gd}} = 0.06$ (\square), 0.04 (\circ), 0.02 (\triangle), 0.009 M (*); (b) reduced transverse and (c) longitudinal ^{17}O relaxation rates; and (d) chemical shifts for $[\text{Gd}_3(\text{H-3taci})_2(\text{H}_2\text{O})_6]^{3+}$ at $B = 14.1$ (\blacksquare), 9.4 (\bullet), 1.41 (\blacktriangle), and 0.572 (\blacklozenge); (e) NMRD profiles at 25 (\blacksquare) and 50 $^\circ\text{C}$ (\bullet). The lines represent the simultaneous least-squares fit to all data points as described in the text.

dipole–dipole and quadrupolar interactions and give direct access to the rotational correlation time of the Gd–O vector (τ_{R}). In the case of the ^{17}O transverse relaxation, the scalar contribution is the most important one. At high fields ($B = 9.4$ and 14.1 T) the $1/T_{2\text{r}}$ values of the $[\text{Gd}_3(\text{H-3taci})_2(\text{H}_2\text{O})_6]^{3+}$ increase with decreasing temperature (Figure 3b), which means that the system is in the fast exchange region, i.e., $1/T_{2\text{r}}$ is

determined by the transverse relaxation rate of the coordinated water oxygen, $1/T_{2\text{m}}$. $1/T_{2\text{m}}$ is influenced by both electronic relaxation rates and water exchange rate. Therefore, to separate these two terms and obtain an exact water exchange rate, one needs independent information on electronic relaxation. At the lowest temperature we start to see the changeover to the slow kinetic region, where $1/T_{2\text{r}}$ is directly determined by the exchange rate, k_{ex} . From the temperature dependence of the binding time ($\tau_{\text{m}} = 1/k_{\text{ex}}$) the activation entropy and enthalpy of the exchange process and the exchange rate at 298.15 K (k_{ex}^{298}) can be calculated.

The chemical shift of the coordinated water oxygen is determined by the hyperfine interaction between the Gd^{3+} electron spin and the ^{17}O nucleus, thus gives access to the value of the hyperfine or scalar coupling constant (A/\hbar).

NMRD. For Gd(III) complexes the measured proton $1/T_1$ relaxation rate is a sum of inner- and outer-sphere contributions.³² The inner-sphere contribution, the relaxivity due to the proton of the exchangeable water molecule bound in the inner coordination sphere, is influenced by correlation times involving rotation, water exchange, and electronic relaxation, as well as the Gd–H distance and the number of inner-sphere water molecules. The outer-sphere contribution, which arises from the relative diffusional motions of unbound water molecules and the Gd^{3+} ion, is influenced by correlation times involving diffusional and electronic relaxation and the distance of closest approach between a water proton and the Gd^{3+} ion. The diffusional motion is characterized by the diffusion constant, D_{GdH} and its activation energy, E_{GdH} . Both inner- and outer-sphere contributions have the electronic relaxation correlation times as common parameters.

Unified Treatment of EPR, ^{17}O NMR, and NMRD Data.

There are a large number of parameters that influence the experimental data obtained by each of the three techniques. One can take advantage of the fact that several of these parameters are common to two or the three techniques, and perform a global fit of all the experimental data with all the equations that describe their influence. This unified treatment leads to more reliable results, since they are determined by several techniques at the same time. It may represent an advantage especially in determining the parameters that describe electronic relaxation, which influences EPR, ^{17}O NMR, and NMRD. It is also very useful to cover a similar field range in EPR and ^{17}O NMR (in this present study ^{17}O transverse relaxation rates were also obtained at an extreme low field (0.572 T) which is very close to the magnetic field of the X-band EPR measurements (0.34 T)).

The transverse electronic relaxation rates, the reduced ^{17}O transverse and longitudinal relaxation rates and chemical shifts, and the proton relaxivities for $[\text{Gd}_3(\text{H-3taci})_2(\text{H}_2\text{O})_6]^{3+}$ are presented in Figure 3. We performed a simultaneous least-squares fit of the NMRD, EPR, and ^{17}O NMR data in Figure 3 with the following fitted parameters: k_{ex}^{298} (or ΔS^\ddagger), ΔH^\ddagger , A/\hbar , τ_{R}^{298} , E_{R} , τ_{v}^{298} , E_{v} , Δ^2 , and δg^2 . Since there is very often a discrepancy between the τ_{R} values obtained in separate fits of ^{17}O and ^1H NMR data (due to the use of incompatible r_{GdH} and r_{GdO} values), in the simultaneous treatment we fit either the Gd–O distance, r_{GdO} , and fix the quadrupolar coupling constant ($\chi(1 + \eta^2/3)^{1/2} = 7.58$ MHz) or adjust $\chi(1 + \eta^2/3)^{1/2}$ and fix r_{GdO} (2.5 Å). τ_{Re}^{298} and E_{Re} were fixed to values obtained in the fit of the high field EPR data. Due to the absence of a slow kinetic region, we cannot determine the value of the outer-

(32) Koenig, S. H.; Brown, R. D., III. *Prog. Nucl. Magn. Reson. Spectrosc.* **1990**, *22*, 487.

Table 2. Parameters Obtained from the Simultaneous Fitting Procedure of EPR, ^{17}O NMR, and NMRD Data^a

	$[\text{Gd}_3(\text{H}_3\text{-taci})_2(\text{H}_2\text{O})_6]^{3+}$	$[\text{Gd}(\text{PDTA})(\text{H}_2\text{O})_2]^{-b}$	$[\text{Gd}(\text{H}_2\text{O})_8]^{3+c}$
$k_{\text{ex}}/10^6 \text{ s}^{-1}$	11.0 ± 2 (12.0 \pm 2)	102 ± 10	804 ± 60 (830 \pm 95)
$\Delta H^\ddagger/\text{kJ mol}^{-1}$	59.8 ± 3 (60.3 \pm 3)	11 ± 1.4	15.3 ± 1.3 (14.9 \pm 1.3)
$\Delta S^\ddagger/\text{J mol}^{-1}\text{K}^{-1}$	-89 ± 22 (-92 \pm 20)	-54.6 ± 4.6	-23.1 ± 4 (-24.1 \pm 4.1)
$\Delta V^\ddagger/\text{cm}^3 \text{ mol}^{-1}$	-12.7 ± 1.5	-1.5 ± 0.1	-3.3 ± 0.2
$A/\hbar/10^6 \text{ rad s}^{-1}$	-4.5 ± 0.2 (-4.6 \pm 0.2)	-4.94 ± 0.2	-5.3 ± 0.1 (-5.3 \pm 0.2)
C_{os}	<u>0.1</u> (0.1)	<u>0.0</u>	<u>0.0</u> (0.0)
$\tau_{\text{R}}/298/\text{ps}$	37 ± 2 (51 \pm 2)	79 ± 3	41 ± 2 (29 \pm 2)
$E_{\text{R}}/\text{kJ mol}^{-1}$	16.0 ± 1.0 (17.0 \pm 1.0)	19.2 ± 1.1	15.0 ± 1.3 (15.1 \pm 1.5)
$\tau_{\text{v}}/298/\text{ps}$	10.0 ± 1 (6.5 \pm 0.8)	16 ± 2	7.3 ± 0.5 (7.2 \pm 0.7)
$E_{\text{v}}/\text{kJ mol}^{-1}$	7 ± 2 (1 \pm 2)	10.4 ± 2	18.4 ± 1.4 (15.4 \pm 1.1)
$\Delta^2/10^{20} \text{ s}^{-2}$	0.70 ± 0.06 (0.72 \pm 0.04)	0.80 ± 0.04	1.19 ± 0.09 (0.93 \pm 0.04)
$\tau_{\text{Re}}/298/\text{ps}$	<u>0.3</u> (0.3)	—	—
$E_{\text{Re}}/\text{kJ mol}^{-1}$	<u>1.0</u> (1.0)	—	—
$\delta g_{\text{L}}^2/10^{-2}$	3 ± 0.8 (3 \pm 0.8)	—	<u>0.0</u> (0.0)
$\chi(1 + \eta^{2/3})^{1/2}/\text{MHz}$	$7.58/11.7 \pm 0.6$ (<u>7.58</u>)	<u>7.58</u>	$7.58/2.0 \pm 2.3$ (7.58)
$r_{\text{GdO}}/\text{\AA}$	$2.31 \pm 0.03/2.5$ (<u>2.5</u>)	<u>2.5</u>	$2.76 \pm 0.06/2.5$ (<u>2.5</u>)

^a The values in parentheses were obtained by fitting only ^{17}O NMR and EPR data. The underscored parameters were fixed in the fitting procedure.

^b From ref 34. The parameters were obtained from an ^{17}O NMR study. ^c From ref 14.

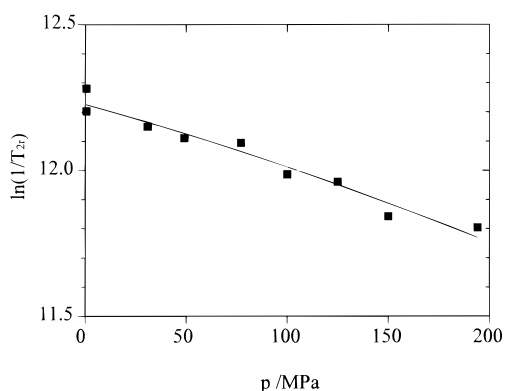


Figure 4. Pressure dependence of the reduced transverse ^{17}O relaxation rates for $[\text{Gd}_3(\text{H}_3\text{-taci})_2(\text{H}_2\text{O})_6]^{3+}$ at 9.4 T and 355.8 K. The line represents the least-squares fit as explained in the text.

sphere constant, C_{os} , that describes the outer-sphere contribution to the ^{17}O chemical shift. Therefore in the fits it was fixed to 0.1, a typical value previously found for Gd(III) complexes.¹⁴ No concentration dependence was found for the reduced transverse and longitudinal ^{17}O relaxation rates and chemical shifts for the complex, thus the $1/T_{1r}$, $1/T_{2r}$, and $\Delta\omega_r$ values measured in solutions of different concentrations were fitted together. As in previous NMRD studies, the distance of closest approach of a water proton to a Gd(III) center, a_{GdH} , was fixed at 3.5 \AA , and the inner-sphere Gd–H distance, r_{GdH} , at 3.1 \AA . The values of the diffusion constant, D_{GdH}^{298} , and its activation energy, E_{GdH} , were fixed to $23 \times 10^{-10} \text{ m}^2 \text{ s}^{-1}$ and 22.0 kJ mol^{-1} , respectively.¹⁴ The resulting curves are shown in Figure 3, and the fitted parameters are listed in Table 2.

Variable-Pressure ^{17}O NMR. The pressure dependence of the reduced transverse relaxation rates, $1/T_{2r}$, for $[\text{Gd}_3(\text{H}_3\text{-taci})_2(\text{H}_2\text{O})_6]^{3+}$ at 355.8 K and 9.4 T is shown in Figure 4. At this temperature and magnetic field, $1/T_{2r}$ is in the fast exchange limit and dominated by the scalar interaction. The decrease of $1/T_{2r}$ with pressure is, therefore, due to an acceleration of the water exchange process. The scalar coupling constant (A/\hbar) was found previously independent of pressure,³³ so we assume that it is constant and equal to the value in Table 2. The mean square deviation of the \mathbf{g}_{L} tensor, δg_{L}^2 , was also assumed to be pressure independent. An activation volume of $+1 \text{ cm}^3 \text{ mol}^{-1}$ (presumably due to changes in microscopic viscosity) was measured for τ_{R} and fixed accordingly. τ_{v} was

assumed to be pressure independent. In fact, ascribing a pressure dependence equivalent to activation volumes between -10 and $+10 \text{ cm}^3 \text{ mol}^{-1}$ to τ_{v} had a negligible effect on the fitted parameters ($<6\%$ on ΔV^\ddagger). The results of the least-squares fit can be seen in Figure 4; the fitted parameters are $(k_{\text{ex}})_0^{356} = (2.4 \pm 0.3) \times 10^7 \text{ s}^{-1}$ and $\Delta V^\ddagger = (-12.7 \pm 1.5) \text{ cm}^3 \text{ mol}^{-1}$.

Discussion

Solution Structure of the $[\text{Ln}_3(\text{H}_3\text{-taci})_2(\text{H}_2\text{O})_6]^{3+}$ Complexes. The X-ray diffraction study of the Gd^{III} -, Eu^{III} -, and La^{III} -taci complexes revealed a very symmetrical structure where each of the metal ions is coordinated to two amines, four deprotonated alkoxo oxygens and two water molecules, resulting in a total coordination number of 8. ^1H NMR studies on the $[\text{Eu}_3(\text{H}_3\text{-taci})_2(\text{H}_2\text{O})_6]^{3+}$ complex in aqueous solution and pH-potentiometric measurements on different lanthanide^{III}-taci complexes showed that species of the same $[\text{Ln}_3(\text{H}_3\text{-taci})_2]^{3+}$ composition are present in solution as well (pH > 6.5).^{9,10} The dysprosium induced shift method resulted in $n = 2.3$ for the number of coordinated water molecules per metal. This number might suggest that there is an equilibrium between differently hydrated ($n = 2, 3$) complexes in solution, which could be reasonable, since the usual coordination number in lanthanide(III) complexes is 8 or 9. However, the temperature invariance of the single absorption band in the UV-vis spectra of $[\text{Eu}_3(\text{H}_3\text{-taci})_2(\text{H}_2\text{O})_6]^{3+}$ lets us unambiguously exclude the presence of any hydration equilibrium in the solution. On the basis of the dysprosium induced shift and the europium UV-vis study it is suggested that the complex has the same $[\text{Ln}_3(\text{H}_3\text{-taci})_2(\text{H}_2\text{O})_6]^{3+}$ structure in solution as in the solid form, i.e., the total coordination number of the metal is 8.

This structure is confirmed by the ^{17}O NMR study of the Gd(III) complex. The scalar coupling constant is a measure of the gadolinium spin density at the oxygen nucleus and also gives an indication on the Gd–OH₂ distance. The value obtained assuming $n = 2$ is very close to the one for $[\text{Gd}(\text{PDTA})(\text{H}_2\text{O})_2]^{-}$, which has a relatively similar inner-sphere structure: six coordination sites of the metal are occupied by the poly(aminocarboxylate) ligand, two by water molecules ($A/\hbar = -4.62 \times 10^6 \text{ rad s}^{-1}$; PDTA⁴⁻ = 1,3-propylenediaminetetraacetate).³⁴ It suggests that the structure with two inner-sphere water molecules is correct. If there were three water molecules

(33) Cossy, C.; Helm, L.; Merbach, A. E. *Inorg. Chem.* **1989**, *28*, 2699.

(34) Micskei, K.; Powell, D. H.; Helm, L.; Brücher, E.; Merbach, A. E. *Magn. Reson. Chem.* **1993**, *31*, 1011.

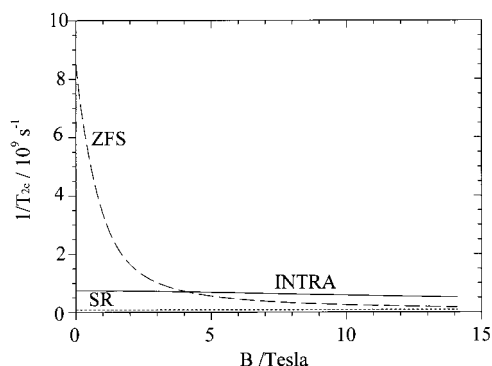


Figure 5. Magnetic field dependence of the different contributions to the overall transverse electronic relaxation rate of $[\text{Gd}_3(\text{H}_{-3}\text{taci})_2(\text{H}_2\text{O})_6]^{3+}$: zero-field splitting mechanism (long dashed line), intramolecular dipole–dipole coupling (straight line) and spin rotation (short dashed line) ($T = 308$ K).

in the inner-coordination sphere, one would obtain from the experimental chemical shift data an unreasonably small value for the scalar coupling constant ($A/\hbar = -3.1 \times 10^6$ rad s^{-1}). The most important piece of evidence for a total coordination number of 8 is the large negative value of the activation volume ($\Delta V^\ddagger = -12.7$ cm^3 mol^{-1}), indicating that the water exchange proceeds via an associatively activated mechanism. For a Gd(III) complex it is only possible if the reactant has a coordination number of 8,³⁵ which confirms that there are two water molecules directly coordinated to the Gd^{3+} .

Electronic Relaxation of $[\text{Gd}_3(\text{H}_{-3}\text{taci})_2(\text{H}_2\text{O})_6]^{3+}$. The fact that the transverse electronic relaxation rates were much larger at high magnetic field for the trimer $[\text{Gd}_3(\text{H}_{-3}\text{taci})_2(\text{H}_2\text{O})_6]^{3+}$ complex than for monomer Gd(III) complexes indicated that intramolecular interactions between the Gd electron spins strongly contribute to relaxation. On the other hand, the absence of a concentration dependence of the relaxation rates indicated that intermolecular effects are negligible. This latter result represents an advantage since the separation of the different contributions to the overall electronic relaxation is simplified: one has only to consider the intramolecular dipole–dipole coupling, the zero-field splitting, and the spin rotation mechanism. The contribution of the three relaxation mechanisms to the transverse electronic relaxation rate as a function of the magnetic field is shown in Figure 5.

The relaxation rate caused by the intramolecular dipole–dipole coupling is slightly decreasing with increasing magnetic field, and becoming the dominant term at $B > 5$ T. High magnetic fields are imperative to the observation of this mechanism.

The zero-field splitting represents a strongly field-dependent contribution, and is dominant at low fields ($B < 5$ T). The parameters describing this mechanism, τ_v^{298} , E_v , and Δ^2 , are determined not only by the EPR data but also by the ^{17}O NMR and NMRD data and were obtained from the simultaneous fit. The correlation time for the modulation of the zero-field splitting, τ_v^{298} , is close to the value obtained for the Gd(III) aqua ion and much shorter than the rotational correlation time of the molecule, as is usually found for Gd(III) complexes. It suggests that the zero-field splitting interaction is modulated by distortions of the coordination sphere and not by rotation. The mean-square zero-field splitting energy, Δ^2 , is higher than that for monomer Gd(III) complexes studied so far (usual values in the range $(0.16\text{--}0.46) \times 10^{20}$ s^{-2}). Perhaps this is an

indication of the decreased symmetry around the metal ion in $[\text{Gd}_3(\text{H}_{-3}\text{taci})_2(\text{H}_2\text{O})_6]^{3+}$ compared to the poly(aminocarboxylate) complexes.

The spin rotation mechanism represents a very small and field-independent contribution to the overall electron spin relaxation.

The presence of a second and a third spin near the one observed provides dipolar relaxation pathways through fluctuations of the distances between them or through reciprocal reorientation. The correlation time of this intramolecular interaction (τ_{Re}) will be the time constant of this process, whatever fluctuation modulates the coupling.³⁶ Hence, the correlation time may give some indication on the nature of the fluctuation that operates in the specific case. The correlation time for the intramolecular interaction that we obtain from the fit of the high field EPR data is much shorter than those for the two Gd(III) dimers studied so far (Table 1). For these dimers the τ_{Re} values were in the range of the rotational correlation time, thus the intramolecular dipole–dipole coupling was explained in terms of a rotational effect. Certainly, we cannot speak about rotation with a correlation time of 0.3 ps. We assume that for the trimer $[\text{Gd}_3(\text{H}_{-3}\text{taci})_2(\text{H}_2\text{O})_6]^{3+}$ complex the observed intramolecular dipole–dipole coupling is the result of a vibrational effect, which could also explain the very small value of the activation energy.

Water Exchange Kinetics. The majority of the Gd(III) complexes studied so far by ^{17}O NMR were nine-coordinate poly(aminocarboxylates) with one inner-sphere water molecule, due to their practical importance as potential MRI contrast agents. During the past few years a substantial body of knowledge has been amassed on how small structural changes in the ligand affect the rate and mechanism of water exchange on Gd(III) poly(aminocarboxylates),^{14,37–39} while little is known about other types of Gd(III) complexes.

The parameters describing water exchange on $[\text{Gd}_3(\text{H}_{-3}\text{taci})_2(\text{H}_2\text{O})_6]^{3+}$ are presented and compared to those of $[\text{Gd}(\text{H}_2\text{O})_8]^{3+}$ and $[\text{Gd}(\text{PDTA})(\text{H}_2\text{O})_2]^-$ in Table 2. The water exchange is 10 times faster on $[\text{Gd}(\text{PDTA})(\text{H}_2\text{O})_2]^-$ than on $[\text{Gd}_3(\text{H}_{-3}\text{taci})_2(\text{H}_2\text{O})_6]^{3+}$ and the aqua ion undergoes the fastest exchange. The mechanism, as determined from the activation volume, has a strong associative activation mode (I_a or A) for $[\text{Gd}_3(\text{H}_{-3}\text{taci})_2(\text{H}_2\text{O})_6]^{3+}$, with the largest negative activation volume ever found for a Gd(III) complex. This volume is practically equal to the limiting value that can be calculated for water exchange on a $[\text{Ln}(\text{H}_2\text{O})_8]^{3+}$ ion through a purely associative mechanism (-12.9 cm^3 mol^{-1}).⁴⁰ For $[\text{Gd}(\text{H}_2\text{O})_8]^{3+}$ and $[\text{Gd}(\text{PDTA})(\text{H}_2\text{O})_2]^-$ the water exchange process has much less associative character ($\Delta V^\ddagger = -3.3$ and -1.5 cm^3 mol^{-1} , respectively), the bond-breaking for the leaving and the bond-formation for the incoming water molecule are practically synchronous processes. The large difference in the activation volumes for $[\text{Gd}_3(\text{H}_{-3}\text{taci})_2(\text{H}_2\text{O})_6]^{3+}$ and $[\text{Gd}(\text{PDTA})(\text{H}_2\text{O})_2]^-$, though their inner-sphere structures are relatively similar, can be explained in terms of steric crowding around the metal ion. In $[\text{Gd}_3(\text{H}_{-3}\text{taci})_2(\text{H}_2\text{O})_6]^{3+}$ the deprotonated alkoxide oxygens

(35) Powell, D. H.; Favre, M.; Graeppli, N.; Ni Dhubhghaill, O. M.; Pubanz, D.; Merbach, A. E. *J. Alloys Compd.* **1995**, 225, 246.

(36) Banci, L.; Bertini, I.; Luchinat, C. *Nuclear and Electron Relaxation*; VCH: Weinheim, 1991.

(37) Tóth, É.; Pubanz, D.; Vauthey, S.; Helm, L.; Merbach, A. E. *Chem. Eur. J.* **1996**, 2, 209.

(38) Tóth, É.; Burai, L.; Brücher, E.; Merbach, A. E. *J. Chem. Soc., Dalton Trans.* **1997**, 1587.

(39) Lammers, H.; Maton, F.; Pubanz, D.; van Laren, M. W.; van Bekkum, H.; Merbach, A. E.; Peters, J. A.; Müller, R. N. *Inorg. Chem.* **1997**, 36, 2527.

(40) Swaddle, T. W. *Adv. Inorg. Bioinorg. Mech.* **1983**, 2, 95.

are probably closer to the Gd^{3+} ion than the carboxylate oxygens in $[\text{Gd}(\text{PDTA})(\text{H}_2\text{O})_2]^-$. However, a carboxylate is a bulkier group than an alkoxide, and as a result, the inner sphere of the $[\text{Gd}(\text{PDTA})(\text{H}_2\text{O})_2]^-$ is sterically more crowded, thus the activation volume is smaller. Another factor that can partly account for the different water exchange mechanisms is the different charge of the two complexes. The positive charge of the Gd^{3+} ion is much less shielded in the $[\text{Gd}_3(\text{H}_{-3}\text{taci})_2(\text{H}_2\text{O})_6]^{3+}$ complex compared to $[\text{Gd}(\text{PDTA})(\text{H}_2\text{O})_2]^-$ and favors the formation of a relatively more stable, nine-coordinate intermediate.

The slower exchange on $[\text{Gd}(\text{PDTA})(\text{H}_2\text{O})_2]^-$ as compared to $[\text{Gd}(\text{H}_2\text{O})_8]^{3+}$ was explained with the less associative character of the process: the participation of the incoming water is less significant in the bond breaking between the leaving water molecule and the metal ion. According to this logic, $[\text{Gd}_3(\text{H}_{-3}\text{taci})_2(\text{H}_2\text{O})_6]^{3+}$ should undergo a very fast water exchange. Evidently, there are other factors that have an important role in this case.

The slower exchange and the larger activation enthalpy indicates that more energy is needed for $[\text{Gd}_3(\text{H}_{-3}\text{taci})_2(\text{H}_2\text{O})_6]^{3+}$ to achieve a nine-coordinate transition state. It is not surprising if one considers that the transition from the eight-coordinate ground state to the nine-coordinate transition state requires a conformational change of the complex. This conformational change requires very little energy for the $[\text{Gd}(\text{H}_2\text{O})_8]^{3+}$, since this aqua ion is adjacent to the region where the coordination number of the lanthanides changes from 8 to 9.⁴¹ $[\text{Gd}_3(\text{H}_{-3}\text{taci})_2(\text{H}_2\text{O})_6]^{3+}$ is a very rigid molecule compared to $[\text{Gd}(\text{H}_2\text{O})_8]^{3+}$ or even $[\text{Gd}(\text{PDTA})(\text{H}_2\text{O})_2]^-$. The conformational change, which can be the rate-determining step in the water exchange for $[\text{Gd}_3(\text{H}_{-3}\text{taci})_2(\text{H}_2\text{O})_6]^{3+}$, is probably a slow process, and consequently, this complex will undergo a relatively slow water exchange. The flexibility, and hence the reactivity, of $[\text{Gd}(\text{PDTA})(\text{H}_2\text{O})_2]^-$ represents an intermediate case between $[\text{Gd}(\text{H}_2\text{O})_8]^{3+}$ and $[\text{Gd}_3(\text{H}_{-3}\text{taci})_2(\text{H}_2\text{O})_6]^{3+}$. However, the exchange on $[\text{Gd}_3(\text{H}_{-3}\text{taci})_2(\text{H}_2\text{O})_6]^{3+}$ is still faster compared to the dissociatively activated water exchange process on the nine-coordinate $[\text{Gd}(\text{DOTA})(\text{H}_2\text{O})]^-$ or $[\text{Gd}(\text{DTPA})(\text{H}_2\text{O})]^{2-}$.¹⁴

Rotation. In our analysis the rotational correlation time can be obtained from the longitudinal ^{17}O and ^1H relaxation rates. When they are treated simultaneously, a single τ_R is fitted which we attribute to the rotation of the Gd–water vector. In this treatment we also fit either the Gd–O distance (the quadrupolar coupling constant is fixed) or the quadrupolar coupling constant (the Gd–O distance is fixed). The value of the Gd–O distance obtained (2.31 Å) is shorter than the one determined in the solid X-ray structure of $[\text{Gd}_3(\text{H}_{-3}\text{taci})_2(\text{H}_2\text{O})_6]\text{Cl}_3 \cdot 3.5\text{H}_2\text{O}$ (2.42–2.46 Å), while the fitted value of the quadrupolar coupling constant is considerably higher than that of the pure water (7.58 MHz), which is reasonable according to a recent study on paramagnetic complexes.⁴² In reality, probably both r_{GdO} and the coupling constant deviate from their value of 2.5 Å and 7.58 MHz, respectively.

Both ^{17}O NMR and NMRD have the same drawback as far as the absolute value of τ_R is concerned: one has to have a good estimation of the Gd–O or Gd–H distance, which are not known in solution. The τ_R obtained from ^{17}O data also depends on the quadrupolar coupling constant ($\chi(1 + \eta^2/3)^{1/2}$), which is also not easily accessible by independent methods. However, when the same Gd–O distance and coupling constant are used

for a series of similar complexes, which is a reasonable approach, one can have a good comparison of the rotational correlation times as determined from oxygen longitudinal relaxation rates. The main advantage of ^{17}O NMR over NMRD is that outer-sphere contributions do not need to be accounted for, whereas in NMRD the separation of the inner- and outer-sphere terms is usually not without difficulty. Consequently, it is more appropriate to compare rotational correlation times as calculated from longitudinal ^{17}O relaxation rates, though, due to the practical importance, MRI contrast agents are usually characterized by the τ_R values obtained from NMRD.

$[\text{Gd}_3(\text{H}_{-3}\text{taci})_2(\text{H}_2\text{O})_6]^{3+}$ has a very short rotational correlation time (51 ps), which is especially surprising when compared to $[\text{Gd}(\text{PDTA})(\text{H}_2\text{O})_2]^-$. Even if we assume that the Gd–O distances and the quadrupolar coupling constants are somewhat different for the three complexes, this difference can by no means account for the unexpected order of the rotational correlation times. As it is shown in Chart 1, $[\text{Gd}_3(\text{H}_{-3}\text{taci})_2(\text{H}_2\text{O})_6]^{3+}$ has an extremely compact and almost spherical structure. It is similar to two hydrophobic hemispheres (the two ligands on the top and the bottom of the complex) with a hydrophilic ring between (the Gd^{3+} ions with the coordinated water molecules). Since the hydrophobic part represents the majority of the total surface toward the bulk water, there is only a limited hydration sphere around the complex. We suggest that these two factors, i.e., the spherical structure and large hydrophobic surface of the $[\text{Gd}_3(\text{H}_{-3}\text{taci})_2(\text{H}_2\text{O})_6]^{3+}$ complex are responsible for the unexpectedly fast rotation.

Effect of Increased Electronic Relaxation Rates on Proton Relaxivity. One objective of this study was to answer the following question: can the electronic relaxation, accelerated by intramolecular dipole–dipole coupling, limit proton relaxivity? We have already seen in Figure 5 that the field dependence of the different contributions to the overall electronic relaxation is very different; while the low field relaxation rates are dominated by the zero-field splitting mechanism, this contribution becomes minor at higher magnetic fields. At the fields normally applied in magnetic resonance imaging ($B < 2$ T), the contribution of the intramolecular mechanism to the overall relaxation rate is not dominant. Thus this additional relaxation mechanism cannot have a strong effect on proton relaxivity at the imaging fields that are important from a practical point of view.

To check this point we have computed the proton relaxivities for $[\text{Gd}_3(\text{H}_{-3}\text{taci})_2(\text{H}_2\text{O})_6]^{3+}$ at 37 °C and 20 MHz ($B = 0.47$ T) as a function of the transverse electronic relaxation rate (Figure 6). As the lower curve shows ($\tau_R = 37$ ps, obtained from the simultaneous fit for $[\text{Gd}_3(\text{H}_{-3}\text{taci})_2(\text{H}_2\text{O})_6]^{3+}$), changes in the electronic relaxation rate have no effect on proton relaxivity; for this complex the limiting factor is definitely the rotational correlation time. This is also true of the currently used Gd-based, monomer contrast agents ($[\text{Gd}(\text{DOTA})]^-$, $[\text{Gd}(\text{DTPA})]^{2-}$, or $[\text{Gd}(\text{DTPA-BMA})]$; DOTA = 1,4,7,10-tetrakis(carboxymethyl)-1,4,7,10-tetraazacyclododecane; DTPA = 1,1,4,7,7-pentakis(carboxymethyl)-1,4,7-triazasheptane). However, for slowly rotating complexes the influence of the electronic relaxation rate becomes more important even at low field, as shown by the two upper curves simulating at increasing rotational correlation times.

Conclusion

EPR measurements on the aqueous solution of $[\text{Gd}_3(\text{H}_{-3}\text{taci})_2(\text{H}_2\text{O})_6]^{3+}$ have shown that there is a strong intramolecular dipole–dipole coupling between the Gd electron spins, which,

(41) Lincoln, S.; Merbach, A. E. *Advances in Inorganic Chemistry*; Sykes, A. G., Ed.; Academic Press: New York, 1995; Vol. 42.

(42) Champmartin, D.; Rubini, P. *Inorg. Chem.* **1996**, *35*, 179.

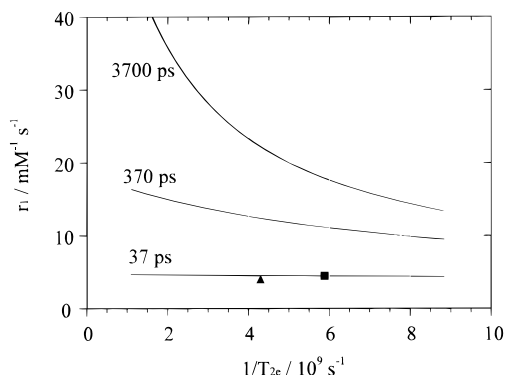


Figure 6. Simulated proton relaxivities (r_1 , per Gd(III)) of $[\text{Gd}_3(\text{H}-3\text{taci})_2(\text{H}_2\text{O})_6]^{3+}$ at 20 MHz proton Larmor frequency and $t = 37^\circ\text{C}$ as a function of the transverse electronic relaxation rate. The actual relaxivities of $[\text{Gd}_3(\text{H}-3\text{taci})_2(\text{H}_2\text{O})_6]^{3+}$ (■) and $[\text{Gd}(\text{DTPA-BMA})]$ (▲) are also shown.

at high magnetic fields, represents a significant contribution to the overall electron spin relaxation. On the basis of its time constant we suggest that this intramolecular interaction is a result of a vibrational effect. At fields used in magnetic resonance imaging the importance of this contribution is negligible compared to the zero-field splitting mechanism, hence it cannot limit proton relaxivity. To our knowledge, this is the first time that intramolecular dipole–dipole interactions in trinuclear Gd(III) complexes, even if only in a phenomenological way, were studied in solution.

The water exchange on $[\text{Gd}_3(\text{H}-3\text{taci})_2(\text{H}_2\text{O})_6]^{3+}$ is about 70 times slower and has much more associative character than on the Gd(III) aqua ion. The large difference in the exchange rate can be explained with the rigidity of the $[\text{Gd}_3(\text{H}-3\text{taci})_2(\text{H}_2\text{O})_6]^{3+}$ which slows down the transition from the eight-coordinate ground state to the nine-coordinate transition state.

The rotational correlation time of the complex is unexpectedly low which was interpreted in terms of a spherical structure with a large hydrophobic surface avoiding the formation of a substantial hydration sphere around $[\text{Gd}_3(\text{H}-3\text{taci})_2(\text{H}_2\text{O})_6]^{3+}$.

Acknowledgment. We are grateful to the Swiss National Science Foundation, the Office for Education and Science (OFES), and to Nycomed Inc. for their financial support. This research was carried out in the frame of the EC COST D8 action and the EU-BIOMED program (MACE Project). We also thank the reviewers for their useful comments.

Supporting Information Available: Tables of variable-temperature reduced transverse and longitudinal ^{17}O relaxation rates and chemical shifts (Tables S.1–S.4); variable-temperature transverse electronic relaxation rates (Table S.5–S.10); proton relaxivities as a function of the magnetic field (Table S.11); and reduced transverse ^{17}O relaxation rates as a function of pressure (Table S.12) are available (6 pages). Ordering information is given on any current masthead page.

Appendix

We give here all the equations that are used in the treatment of ^{17}O NMR and NMRD data.

Oxygen-17 NMR. From the measured ^{17}O NMR relaxation rates and angular frequencies of the paramagnetic solutions, $1/T_1$, $1/T_2$, and ω , and of the acidified water reference, $1/T_{1A}$, $1/T_{2A}$, and ω_A , one can calculate the reduced relaxation rates and chemical shift, $1/T_{1r}$, $1/T_{2r}$, and $\Delta\omega_r$, which may be written as in eqs 10–12,⁴³ where $1/T_{1m}$ and $1/T_{2m}$ are the relaxation rates

of the bound water, $\Delta\omega_m$ is the chemical shift difference between bound and bulk water.

$$\frac{1}{T_{1r}} = \frac{1}{P_m} \left[\frac{1}{T_1} - \frac{1}{T_{1A}} \right] = \frac{1}{T_{1m} + \tau_m} + \frac{1}{T_{1os}} \quad (10)$$

$$\frac{1}{T_{2r}} = \frac{1}{P_m} \left[\frac{1}{T_2} - \frac{1}{T_{2A}} \right] = \frac{1}{\tau_m} \frac{T_{2m}^{-2} + \tau_m^{-1} T_{2m}^{-1} + \Delta\omega_m^2}{(\tau_m^{-1} + T_{2m}^{-1})^2 + \Delta\omega_m^2} + \frac{1}{T_{2os}} \quad (11)$$

$$\Delta\omega_r = \frac{1}{P_m} (\omega - \omega_A) = \frac{\Delta\omega_m}{(1 + \tau_m T_{2m}^{-1})^2 + \tau_m^2 \Delta\omega_m^2} + \Delta\omega_{os} \quad (12)$$

$\Delta\omega_m$ is determined by the scalar coupling constant, A/\hbar , according to eq 13, where B represents the magnetic field.

$$\Delta\omega_m = \frac{g_L \mu_B S(S+1) B A}{3 k_B T \hbar} \quad (13)$$

The outer-sphere contribution to the ^{17}O chemical shift is proportional to $\Delta\omega_m$, where C_{os} is an empirical constant:

$$\Delta\omega_{os} = C_{os} \Delta\omega_m \quad (14)$$

The ^{17}O longitudinal relaxation rates are given by eq 15,^{30,44} where γ_S is the electron and γ_I is the nuclear gyromagnetic ratio ($\gamma_S = 1.76 \times 10^{11} \text{ rad s}^{-1} \text{ T}^{-1}$, $\gamma_I = -3.626 \times 10^7 \text{ rad s}^{-1} \text{ T}^{-1}$), r is the effective distance between the electron charge and the ^{17}O nucleus, I is the nuclear spin ($5/2$ for ^{17}O), χ is the quadrupolar coupling constant and η is an asymmetry parameter:

$$\frac{1}{T_{1m}} = \left[\frac{1}{15(4\pi)} \left(\frac{\mu_0}{r_{\text{GdO}}} \right)^2 \frac{\hbar^2 \gamma_I^2 \gamma_S^2}{r_{\text{GdO}}^6} S(S+1) \right] \times \left[6\tau_{d1} + 14 \frac{\tau_{d2}}{1 + \omega_S^2 \tau_{d2}^2} \right] + \frac{3\pi^2}{10} \frac{2I+3}{I^2(2I-1)} \chi^2 (1 + \eta^{2/3}) \tau_R \quad (15)$$

$$\tau_R = \tau_R^{298} \exp \left[\frac{E_R}{R} \left(\frac{1}{T} - \frac{1}{298.15} \right) \right] \quad (16)$$

In the transverse relaxation the scalar contribution, $1/T_{2sc}$, is the most important one (eq 17).⁴⁵ In eq 17 $1/\tau_{sj}$ is the sum of the exchange rate constant and the electron spin relaxation rate.

$$\frac{1}{T_{2m}} \cong \frac{1}{T_{2sc}} = \frac{S(S+1)}{3} \left(\frac{A}{\hbar} \right)^2 \left(\tau_{s1} + \frac{\tau_{s2}}{1 + \omega_S^2 \tau_{s2}^2} \right) \quad (17)$$

$$\frac{1}{\tau_{sj}} = \frac{1}{\tau_m} + \frac{1}{T_{je}}, \quad j = 1, 2$$

The binding time (or exchange rate, k_{ex}) of water molecules in the inner sphere is assumed to obey the Eyring equation (eq 18), where ΔS^\ddagger and ΔH^\ddagger are the entropy and enthalpy of activation for the exchange process, and k_{ex}^{298} is the exchange rate at 298.15 K.

(45) Micskei, K.; Helm, L.; Brücher, E.; Merbach, A. E. *Inorg. Chem.* **1993**, *32*, 3844.

(46) Bloembergen, N. J. *Chem. Phys.* **1957**, *27*, 572.

(47) Solomon, I. *Phys. Rev.* **1955**, *99*, 559

(48) Koenig, S. H.; Brown, R. D., III. *Prog. NMR Spectrosc.* **1991**, *22*, 487.

(49) Freed, J. H. *J. Chem. Phys.* **1978**, *68*, 4034.

(43) Swift, T. J.; Connick, R. E. *J. Chem. Phys.* **1962**, *37*, 307.

(44) Kowalewski, J.; Nordenskiöld, L.; Betenis, N.; Westlund P.-O. *Prog. Nucl. Magn. Reson. Spectrosc.* **1985**, *17*, 141.

$$\frac{1}{\tau_m} = k_{\text{ex}} = \frac{k_B T}{h} \exp\left\{\frac{\Delta S^\ddagger}{R} - \frac{\Delta H^\ddagger}{RT}\right\} = \frac{k_{\text{ex}}^{298} T}{298.15} \exp\left\{\frac{\Delta H^\ddagger}{R} \left(\frac{1}{298.15} - \frac{1}{T}\right)\right\} \quad (18)$$

The pressure dependence of $\ln(k_{\text{ex}})$ is linear (eq 19), where ΔV^\ddagger is the activation volume and $(k_{\text{ex}})_0^T$ is the water exchange rate at zero pressure and temperature T .

$$\frac{1}{\tau_m} = k_{\text{ex}} = (k_{\text{ex}})_0^T \exp\left\{-\frac{\Delta V^\ddagger}{RT} P\right\} \quad (19)$$

NMRD. The measured proton relaxivities (normalized to 1 mM Gd(III) concentration) contain both inner- and outer-sphere contributions:

$$r_1 = r_{\text{is}} + r_{\text{os}} \quad (20)$$

The inner-sphere term is given by eq 21, where q is the number of inner-sphere water molecules.

$$r_{\text{is}} = \frac{1}{1000} \times \frac{q}{55.55} \times \frac{1}{T_{1m}^H + \tau_m} \quad (21)$$

The longitudinal relaxation rate of inner-sphere protons, $1/T_{1m}^H$ can be expressed as in eq 22:^{46,47}

$$\frac{1}{T_{1m}^H} = \frac{2}{15} \left(\frac{\mu_o}{4\pi}\right)^2 \frac{\hbar^2 \gamma_S^2 \gamma_I^2}{r_{\text{GdH}}^6} S(S+1) \left[\frac{3\tau_{d1}}{1 + \omega_1^2 \tau_{d1}^2} + \frac{7\tau_{d2}}{1 + \omega_S^2 \tau_{d2}^2} \right] \quad (22)$$

In eq 22 r_{GdH} is the effective distance between the Gd(III)

electron spin and the water protons, ω_1 is the proton resonance frequency, and τ_{di} is given by eq 23:

$$\frac{1}{\tau_{di}} = \frac{1}{\tau_m} + \frac{1}{\tau_R} + \frac{1}{T_{ie}}, \quad i = 1, 2 \quad (23)$$

The outer-sphere contribution can be described by eq 24,^{48,49} where N_A is the Avogadro constant, and J_{os} is a spectral density function.

$$r_{\text{os}} = \frac{32N_A \pi (\mu_o)^2}{405} \frac{\hbar^2 \gamma_S^2 \gamma_I^2}{a_{\text{GdH}} D_{\text{GdH}}} S(S+1) [3J_{\text{os}}(\omega_1, T_{1e}) + 7J_{\text{os}}(\omega_S, T_{2e})] \quad (24)$$

$$J_{\text{os}}(\omega, T_{je}) = \text{Re} \left[1 + \frac{1}{4} \left(i\omega \tau_{\text{GdH}} + \frac{\tau_{\text{GdH}}}{T_{je}} \right)^{1/2} \right] \left[1 + \left(i\omega \tau_{\text{GdH}} + \frac{\tau_{\text{GdH}}}{T_{je}} \right)^{1/2} + \frac{4}{9} \left(i\omega \tau_{\text{GdH}} + \frac{\tau_{\text{GdH}}}{T_{je}} \right) + \frac{1}{9} \left(i\omega \tau_{\text{GdH}} + \frac{\tau_{\text{GdH}}}{T_{je}} \right)^{3/2} \right], \quad j = 1, 2 \quad (25)$$

For the temperature dependence of the diffusion coefficient for the diffusion of a water proton away from a Gd(III) complex, D_{GdH} , we assume an exponential temperature dependence, with an activation energy E_{DGdH} :

$$D_{\text{GdH}} = D_{\text{GdH}}^{298} \exp\left\{\frac{E_{\text{DGdH}}}{R} \left(\frac{1}{T} - \frac{1}{298.15}\right)\right\} \quad (26)$$